

AD-A086 006

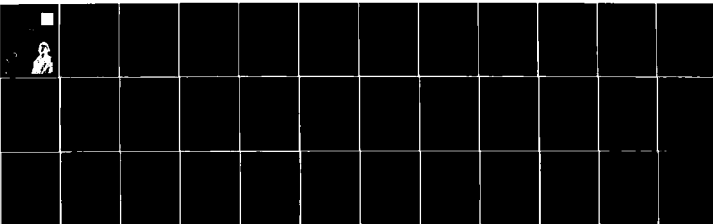
GEORGE WASHINGTON UNIV WASHINGTON D C SCHOOL OF ENGI--ETC F/8 13/13  
A COMPARATIVE STUDY ON THE ELASTIC-PLASTIC COLLAPSE STRENGTH OF--ETC (11)  
FEB 80 R KAO

N00014-75-C-0946

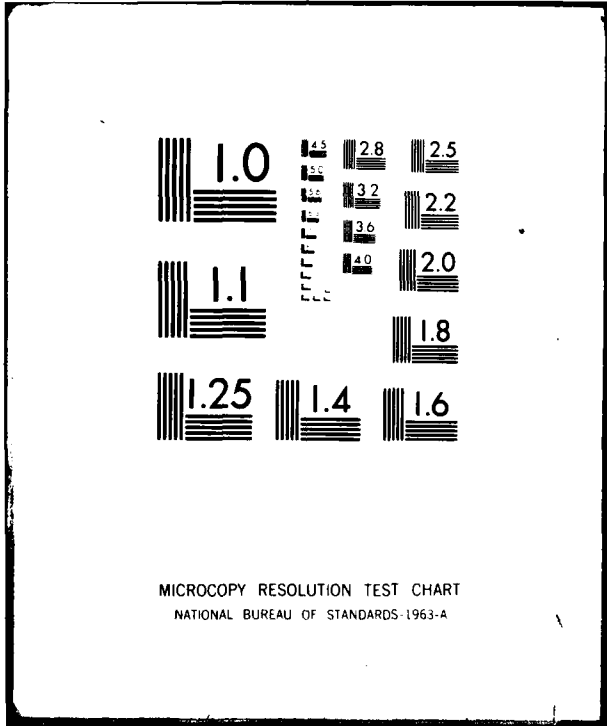
ML

UNCLASSIFIED

Part I  
25-4000



END  
DATE  
FILMED  
8-80  
DTIC



MICROCOPY RESOLUTION TEST CHART  
NATIONAL BUREAU OF STANDARDS-1963-A

12

A COMPARATIVE STUDY ON THE ELASTIC-  
PLASTIC COLLAPSE STRENGTH OF  
INITIALLY IMPERFECT DEEP  
SPHERICAL SHELLS,

THE  
GEORGE  
WASHINGTON  
UNIVERSITY

ADA 086006

LEVEL II

STUDENTS FACULTY STUDY R  
ESEARCH DEVELOPMENT FUT  
URE CAREER CREATIVITY CC  
MMUNITY LEADERSHIP TECH  
NOLOGY FRONTIER DESIGN  
ENGINEERING APP ENC  
GEORGE WASHINGTON UNIV



RECEIVED  
JUN 26 1980

This document has been approved  
for public release and sale; its  
distribution is unlimited.

11 001

SCHOOL OF ENGINEERING  
AND APPLIED SCIENCE

12

6 A COMPARATIVE STUDY ON THE ELASTIC-  
PLASTIC COLLAPSE STRENGTH OF  
INITIALLY IMPERFECT DEEP  
SPHERICAL SHELLS,

11 Robert Kao

142

Sponsored by  
Office of Naval Research  
Arlington, Virginia 22217

Contract Number  
NAVY 00014-75-C-0946

ELECTRIC  
11

11 February 1980

School of Engineering and Applied Science  
The George Washington University  
Washington, D. C. 20052

153370

This document has been approved  
for public release and sale; its  
distribution is unlimited.

JCR

A COMPARATIVE STUDY ON THE ELASTIC-PLASTIC COLLAPSE STRENGTH  
OF INITIALLY IMPERFECT DEEP SPHERICAL SHELLS<sup>1</sup>

By  
Robert Kao



February 1980

<sup>1</sup> The research reported on here was supported by the  
Office of Naval Research, Contract Number  
NAVY 00014-75-C-0946

ABSTRACT

✓  
A finite-difference method for the large deformation elastic-plastic analysis of spherical caps is applied to predict the collapse strength of initially imperfect deep spherical shells. Twelve uniformly loaded hemispherical shell models with flat spots at their apex are analyzed. For each model, a number of shallow spherical regions containing the flat spot are selected from its domain. One of these selected shallow regions yields a minimum buckling pressure; this minimum value is taken as the theoretical buckling load for the shell model under consideration. Present solutions are in good agreement with existing experimental and empirical results. The good comparison suggests that initially imperfect deep spherical shells may be analyzed by using a much simpler mathematical model - the spherical cap, and thus the analytical cost may be greatly reduced. This also demonstrates that the collapse of imperfect spherical shells is primarily a local phenomenon and therefore dependent on local geometry. Consequently, the presence of initial imperfections must be fully taken into consideration in any large deformation inelastic buckling analysis before such analysis can be expected to quantitatively predict the collapse strength of practical shell structures.



P-1

Accession For	<input checked="" type="checkbox"/>
NTIS GRA&I	
DOC TAB	
Unannounced	
Justification	
By	
Distribution/	
Availability Codes	
Avail and/or special	
Dist	A

## INTRODUCTION

Buckling analysis of spherical shell structures has received considerable attention in the literature. This may be attributed to the fact that the use of spherical shells to resist uniform external hydrostatic pressure has increased rapidly in recent years. This increased use results from the introduction of missiles and other spacecrafts and also from the growing interest in hydrospace.

Timoshenko [1] summarized the classical small deflection theory for the elastic buckling of a complete spherical shell. Unfortunately, earlier tests conducted in Ref. [2] provided only one-fourth of the collapse strength predicted by the classical buckling theory. The huge discrepancy existed between the theory and the test is traceable. The test specimens used in Ref. [2] were formed from flat plates, which inevitable introduced significant departures from sphericity as well as variations in thickness and residual stresses. Since the initial imperfection among these adverse factors introduced has been assumed to be the primary source that affects the collapse strength of shell structures [3-6], the discrepancy is consequential and their comparison is inappropriate.

To eliminate or at least partially reduce the adverse effect from flat plates, a series of nearly perfect machined shells were made in Refs. [7-9]. The test results showed their collapse

strength was nearly 90% of the classical buckling pressure. These tests not only provide a strong support to the classical small deflection buckling theory of initially perfect spherical shells, but indicate that the initial imperfection does play a significant role in reducing shell load-carrying capacity.

In view of the practicality, it is very difficult, if not impossible, to manufacture or measure most spherical shells with sufficient accuracy to justify the use of classical shell buckling formulas in design. It thus becomes evident that we should consider the unevenness factors in the shell buckling analysis. Since most contributions to the unevenness factors, such as variation in thickness, residual stress, boundary conditions, etc. may be, at least on occasions, are fairly well controllable, the effect of initial departures from sphericity appears most worthy of investigation.

In connection with this investigation, the large deflection elastic buckling analysis was performed in Ref. [5] for complete spherical shells with a dimple type of initial imperfections. Focused only on shallow spherical portions of these complete shells, numerical solutions of these modified shell structures [6] compare quite satisfactorily with those of [5].

The comparison by itself prompts a basic assumption that the collapse of initially imperfect shell structures is primarily a local phenomenon and therefore critically dependent on local geometry.

For the purpose of the same investigation with an extension

to include both elastic and inelastic behavior, 62 machined hemispherical shell models with local thin spots and flat spots and subjected to uniform external hydrostatic pressure were tested in Ref. [3]. Based on the classical buckling equation, empirical formulas were also proposed in the same reference, using local geometry rather than nominal shell dimensions to account for the effect of initial imperfections on the collapse strength. Buckling loads obtained from both experiments and empirical formulas are in good agreement. This good agreement lends a strong support to the validity of the aforementioned basic assumption.

By adopting the same basic assumption, the computer program developed in Ref. [4] for the large deformation elastic-plastic buckling analysis of spherical caps is utilized in this report to predict the collapse strength of those hemispherical shells with flat spots in Ref. [3]. The present analysis has following purposes. First, through a comparison of present analytical solutions with empirical and test results of [3], it is intended to verify the validity of the computer code developed in Ref. [4]. Secondly, it is attempted to illustrate the degree of reliability of the spherical cap theory when it is applied to predict the collapse strength of initially imperfect deep spherical shells in both elastic and inelastic behavior. Finally, we also intend to demonstrate the usefulness of the spherical cap theory by its applications. The final purpose is, in effect, to justify the efforts of numerous research activities as have been done so far for the development of the shallow spherical shell theory.

## LARGE DEFORMATION ELASTIC-PLASTIC THIN SPHERICAL CAP THEORY

### Governing Equations

As mentioned in the previous Section, the large deformation elastic-plastic thin shallow spherical shell theory [4] is utilized in this paper to predict the collapse strength of initially imperfect deep spherical shells. A shell is called "thin" if the ratio of its thickness to the radius of curvature of its middle surface is much less than unity; and a spherical shell is called "shallow" if its rise at the center is less than, say, one-eighth of its base diameter.

The geometry of a clamped spherical cap is shown in Fig. 1(a), in which  $H$  is the central height,  $R$  the shell radius to the midsurface of the shell,  $a$  the base radius, and  $h$  the shell thickness;  $W(r)$  and  $U(r)$  are displacement components along normal and tangential directions, respectively, and  $W_i(r)$  is the initial imperfection;  $q$  is the applied uniform pressure. Also shown in Fig. 1(b) are membrane forces  $N_r$  and  $N_\theta$ , the transverse shear  $Q_r$  and moments  $M_r$  and  $M_\theta$ .

In view of the axisymmetric nature of the problem encountered here (Fig. 1), we need only consider the situation along a generic radius. Governing equations of this problem have been derived in a great detail in Ref. [4], only a summary of these equations will be given here. For convenience, let's first introduce following nondimensional quantities:

$$\begin{aligned}
 x &= r/a & m^4 &= 12(1-\nu^2) \\
 \lambda^2 &= m^2 a^2 / Rh & q_{CR} &= 4Eh^2 / R^2 m^2 \\
 ( )' &= \partial( ) / \partial x & p &= q / q_{CR} \\
 u &= a U / h^2 & w_i &= W_i / h \\
 w &= W / h
 \end{aligned}
 \tag{1}$$

where E is Young's modulus,  $\nu$  is Poisson's ratio, and  $q_{CR}$  is the classical buckling pressure of a complete sphere of the same radius of curvature and thickness;  $\lambda$  is a spherical cap geometric parameter.

Governing equations in terms of these nondimensional quantities are written as follows:

$$u'' + \frac{u'}{x} - \frac{u}{x^2} + g(w) = \frac{(1-\nu^2)a^3}{Eh^3} q_1^p \tag{2}$$

$$\begin{aligned}
 \nabla^4 w - 12(\epsilon_r + \nu\epsilon_\theta) \left( w_f'' + \frac{\lambda^2}{m^2} \right) - 12(\epsilon_\theta + \nu\epsilon_r) \left( \frac{w_f'}{x} + \frac{\lambda^2}{m^2} \right) \\
 = 4 \frac{\lambda^4}{m^2} p - \frac{m^4 a^4}{Eh^4} (q_2^p + q_3^p)
 \end{aligned}
 \tag{3}$$

where

$$g(w) = f_r'(w) + \nu f_\theta'(w) + (1-\nu)[f_r(w) - f_\theta(w)]/x$$

$$f_r(w) = - \frac{\lambda^2}{m^2} w + \frac{1}{2}(w')^2 + w'w_i$$

$$f_{\theta}(w) = -\frac{\lambda^2}{m^2} w$$

$$f_r'(w) = -\frac{\lambda^2}{m^2} w' + w'w'' + w'w_i'' + w''w_i'$$

$$f_0'(w) = -\frac{\lambda^2}{m^2} w' \quad (4)$$

$$\epsilon_r = u' - \frac{\lambda^2}{m^2} w + \frac{1}{2}(w')^2 + w'w_i''$$

$$\epsilon_{\theta} = \frac{u}{x} - \frac{\lambda^2}{m^2} w$$

$$w_f = w + w_i \quad \nabla^2(\ ) = (\ )'' + (\ )'/r$$

$$q_1^p = (N_r^p)' + N_r^p/r - N_{\theta}^p/r$$

$$q_2^p = N_r^p(w_f'' + 1/R) + N_{\theta}^p(w_f'/r + 1/R)$$

$$q_3^p = (M_r^p)'' + 2(M_r^p)'/r - (M_{\theta}^p)'/r$$

$q_i^p$  in these expressions are effective plastic forces. Effective plastic membrane forces  $N_r^p$ ,  $N_{\theta}^p$ , and effective plastic moments  $M_r^p$ ,  $M_{\theta}^p$  are expressed in integral forms of plastic strains  $e_r^p$  and  $e_{\theta}^p$ :

$$\begin{Bmatrix} N_r^p \\ N_{\theta}^p \end{Bmatrix} = [E] \int_{-h/2}^{h/2} \begin{Bmatrix} e_r^p \\ e_{\theta}^p \end{Bmatrix} dz$$

$$\begin{Bmatrix} M_r^p \\ M_\theta^p \end{Bmatrix} = [E] \int_{-h/2}^{h/2} \begin{Bmatrix} e_r^p \\ e_\theta^p \end{Bmatrix} z dz \quad (5)$$

$$[E] = \frac{E}{1-\nu^2} \begin{bmatrix} 1 & \nu \\ \nu & 1 \end{bmatrix}$$

where  $z$  is the vertical coordinate through the shell thickness (Fig. 1b).

Boundary condition at outer edge of the spherical cap is assumed to be clamped which requires:  $u(1) = w(1) = w'(1) = 0$ . Due to symmetry at apex, we also have  $u(0) = w'(0) = 0$ .

#### Constitutive Equations of Plasticity

The flow rule of von Mises and the Ziegler-Prager kinematic hardening rule are selected to describe the inelastic material property in this study. This selection has the advantage that the Bauschinger effect is properly accounted for. In the incremental solution procedure for elastic-plastic problems, it is required to define constitutive relations and loading criteria.

To begin with, let's discuss loading criteria. For this purpose, it needs to introduce  $\dot{f} = (\partial f / \partial \sigma_{ij}) d \sigma_{ij}$ , where  $f = 0$  is the yield surface,  $\sigma_{ij}$  is stress vector, and  $\alpha_{ij}$  is the position vector of the yield surface center  $C$  which before plastic deformation takes place is located at the origin. For the case of plane stress (Fig. 2),  $f$  takes the form

$$f = \bar{\sigma}_1^2 - \bar{\sigma}_1 \bar{\sigma}_2 + \bar{\sigma}_2^2 - \sigma_y^2 = 0 \quad (6)$$

where  $\sigma_y$  is the yield stress in uniaxial tension and  $\bar{\sigma}_1 = \sigma_1 - \alpha_1$ ,  $\bar{\sigma}_2 = \sigma_2 - \alpha_2$ . Loading, unloading and neutral loading are associated with the plastic state  $f = 0$ , and are characterized by  $\dot{f} > 0$ ,  $\dot{f} < 0$  and  $\dot{f} = 0$ , respectively.

For a shell deforming into a plastic range, the total strain in a point within the thickness can be considered as a combination of its elastic and plastic components:

$$\{e\} = \{e^e\} + \{e^p\} \quad (7)$$

When loading or neutral loading takes place, stress increments are simply expressed in terms of total strain increments [4] as follows:

$$\begin{Bmatrix} \Delta\sigma_1 \\ \Delta\sigma_2 \end{Bmatrix} = \begin{bmatrix} C_{11} & C_{12} \\ C_{21} & C_{22} \end{bmatrix} \begin{Bmatrix} \Delta e_1 \\ \Delta e_2 \end{Bmatrix} \quad (8)$$

where

$$C_{11} = \frac{E}{\Omega}(D + E S_2^2)$$

$$C_{12} = \frac{E}{\Omega}(D\nu - ES_1 S_2) = C_{21}$$

$$C_{22} = \frac{E}{\Omega}(D + E S_1^2)$$

$$\Omega = D(1 - \nu^2) + E(S_1^2 + 2\nu S_1 S_2 + S_2^2)$$

$$S_1 = (\bar{\sigma}_1 - \bar{\sigma}_2/2)/\sigma_y, \quad S_2 = (\bar{\sigma}_2 - \bar{\sigma}_1/2)/\sigma_y, \quad D = \frac{\Delta\sigma}{\Delta e^p}$$

Expression for D implies that its value is equal to the slope of the uniaxial stress-plastic strain curve.

Figure 3 shows three types of hardening, the D value associated with each of them may be given here: (i) for an elastic-ideally plastic material,  $D = 0$ , (ii) for a linear hardening material,  $D = EE_t/(E-E_t)$ , where  $E_t$  is the tangent modulus, (iii) for the case of nonlinear hardening, the expression of D, which is obtained on the basis of the Ramberg-Osgood representation for a uniaxial nonlinear stress-strain curve, is omitted here. Because of requiring a rather lengthy interpretation, readers are referred to Ref. [4] for this expression.

For a material point whose stresses are still in an elastic range or in an unloading situation, Hook's Law should be applied:

$$\begin{Bmatrix} \Delta\sigma_1 \\ \Delta\sigma_2 \end{Bmatrix} = \frac{E}{1-\nu^2} \begin{bmatrix} 1 & \nu \\ \nu & 1 \end{bmatrix} \begin{Bmatrix} \Delta e_1^e \\ \Delta e_2^e \end{Bmatrix} \quad (9)$$

### Solution Procedure

For convenience, a simple flow chart is sketched in Fig. 4 to explain the general solution procedure. The entire process is divided into two major loops, namely, the elastic solution and material property loops.

In the elastic solution loop, all material properties are held constant, the effective plastic loads  $q_i^p$  are fixed and combined with the applied load  $q$ . The problem is thus reduced

to an elastic large deformation problem. The solution plan to this problem is to superpose a finite-difference mesh on the one-dimensional shell domain, replace nonlinear differential equations by a set of two nonlinear algebraic finite-difference equations, and solve the resulting set of equations by the nonlinear relaxation method [10].

In the material property loop, effective plastic load terms are updated so that their values correspond to the computed state of stress and to the specified nonlinear stress-strain relation at all points over the shell surface and throughout the shell thickness.

Iterations keep going back and forth on these two loops until the specified material property and equilibrium equations are simultaneously satisfied. For more detailed information on the solution procedure outlined here, readers are referred to Ref. [4].

EMPIRICAL FORMULAS FOR THE COLLAPSE STRENGTH OF IMPERFECT DEEP  
SPHERICAL SHELLS

Based on many experimental results, Krenzke and Kiernan [3] proposed empirical formulas for the calculation of the collapse strength of initially imperfect spherical shells. These equations are essentially the modifications of the classical buckling equation for a complete spherical shell [1], taking into account the limitations of realistic fabrication techniques and the effects of initial departures from sphericity and thickness variations on the elastic or inelastic collapse strength.

For convenience, we shall first list the classical buckling equation of a complete sphere and empirical formulas for the elastic and inelastic collapse strength of near-perfect spherical shells. By assuming  $\nu = 0.3$ , these equations of interest are given as follows:

$$q_{cr} = 1.21 E(h/R)^2 \quad (10)$$

$$q_1 = 0.7 q_{cr} = 0.84 E(h/R_0)^2 \quad (11)$$

$$q_E = 0.84 \sqrt{E_s E_t} (h/R_0)^2 \quad (12)$$

where  $R_0$  is the outer radius of the sphere. Equation (10) is the classical buckling equation of a complete spherical shell as already given in Eq. (1) ( $R$  in this equation is the radius

to the midsurface of the shell).

Considering the difficulty involved in manufacturing or measuring most spherical shells with sufficient accuracy to justify the use of the classical equation in design, it is suggested in Ref. [3] that Eq. (10) be replaced by Eq. (11) for calculating the buckling strength of near perfect spheres. Eventually Eq. (11) states that near-perfect spheres collapse at about 0.7 times the classical strength.

A similar formula, Eq. (12), is also proposed for predicting the inelastic buckling strength of near-perfect spheres. The secant and tangent moduli used in Eq. (12) are derived from the typical uniaxial tension or compression stress-strain curve. A shell is considered to be nearly perfect if the ratio of its maximum imperfection  $(W_i)_{\max}$  to its wall thickness  $h$  is less than 2 to 3 percent.

Before going to list empirical formulas for the collapse strength of imperfect spherical shells, we shall here introduce a so called "critical arc length" --  $L_c$ . By taking a  $\lambda$  value of 2.2\* and  $a$  (spherical cap base radius) equal to  $L_c/2^{**}$ ,  $L_c$  can be obtained from  $\lambda$  expression of Eq. (1) as follows:

$$L_c = 2.42\sqrt{R_1 h_a} \quad (13)$$

---

\*From theoretical and experimental results of spherical caps, for  $\lambda$  values greater than approximately 2.2, the detrimental effect of clamping the edges diminishes as the shells become more stable; see Ref. [3].

\*\*Because of the assumed shallowness, the cord length is approximated by the arc length.

in which  $h_a$  and  $R_1$  are the average shell thickness and the local radius to the midsurface of the shell over a critical arc length associated with a  $\lambda$  value of 2.2.

Empirical formulas for the collapse strength of initially imperfect spherical shells can now be readily obtained from expressing Eqs. (11-12) in terms of local geometry:

$$q_1' = 0.84 E (h_a/R_{10})^2 \quad (14)$$

$$q_E' = 0.84 \sqrt{E_s E_t} (h_a/R_{10})^2 \quad (15)$$

where  $R_{10}$  is the local radius to the outside surface of the shell over a critical arc length associated with a  $\lambda$  value of 2.2.

The primes in Eqs. (14-15) simply imply that the local geometry is used to calculate the buckling pressure. In fact, Eq. (15) may be used to compute the buckling strength of initially imperfect spheres which collapse in either the elastic or inelastic region, since Eq. (15) reduces to Eq. (14) in the elastic region.

These formulas are essentially "engineering type" solutions and do not intend to be regarded as a theoretical treatment of the strength analysis of imperfect spherical shells. The effect of initial deviations from sphericity is extremely important in both elastic and inelastic buckling cases, because the local radius appears in their buckling equations to the second power.

## EXPERIMENT

Series FS models experimented in Ref. [3] are selected in this paper for the purpose of verifying the theoretical work. This series of models was designed to study the effect of local imperfections on the hydrostatic collapse strength of deep epherical shells which collapse in either the elastic or inelastic region.

Series FS consists of 36 machined models of hemispherical shells with local flat spots as shown in Fig. 5. All models have the same inner diameter of 1.625 inches. Each model has nearly uniform wall thickness, however, dimensions of the wall thickness are different from model to model. The flat spots, which were machined in the apex of each model, have an included angle of  $10^\circ$  for models FS-1 through FS-9,  $20^\circ$  for models FS-10 through FS-27, and  $30^\circ$  for models FS-28 through FS-36. The local radius of curvature is held constant for each flat spot and is about 1.15 times the nominal radius for Models FS-10 through FS-18 and about 1.4 times the nominal radius for all remaining models.

Each model was machined in an identical manner. The interior contours were machined by use of form tools, the exterior contours by supporting the inside contours on a mating mandrel and by generating the outside surface using a lathe with a ball-turning attachment.

The model dimensions are given in Table 1. These models

were machined from 7075-T6 aluminum bar stock whose stress-strain curve was displayed in Fig. 6. For simplicity in analysis, the nonlinear material hardening behavior is approximated with a linear hardening:  $E$  (Young's modulus) =  $10.8 \times 10^6$  psi,  $E_t$  (tangent modulus) =  $1.1 \times 10^6$  psi and  $\sigma_y$  (initial yield stress) =  $7.8 \times 10^4$  psi. As already mentioned, a Poisson's ratio  $\nu$  of 0.3 in the elastic range is assumed for all models.

Each model was tested under external hydrostatic pressure. Pressure was applied in increments and each new pressure level was held at least 1 minute. The final pressure increment was always less than 2 percent of the maximum pressure. Every effort was made to minimize any pressure surge when applying pressure.

THEORETICAL SOLUTIONS AND COMPARISON WITH EMPIRICAL AND  
EXPERIMENTAL RESULTS

The large deformation elastic-plastic spherical cap theory outlined in an earlier section is applied here for the buckling analysis of initially imperfect hemispherical shells. Hemispherical shells considered here are those of 36 Series FS models tested in Ref. [3]. These shell structures have flat spots at their apex. As has been mentioned in the previous section, the material property and shell geometry are given in Fig. 6 and Table 1, respectively.

Figure 7 shows a clamped spherical cap which is produced from a hemispherical shell. It is noted that the spherical cap selected is well beyond the flat spot region to fully account for the effect of the entire initially imperfect region. The included angle and radius of curvature to the midsurface are  $\beta$  and  $R$  for the entire spherical cap,  $\alpha$  and  $R_1$  for the flat spot, and  $\phi$  and  $R$  for the perfect portion occupied by the flat spot. All radii mentioned here are referred to the midsurface of the shell.

An immediate question should be raised here: what is the appropriate size of a spherical cap to be selected? The answer to this question may have to resort to the requirement for a spherical cap. The assumed shallowness - the rise at the cap center is less than one-eighth of its base diameter - asks for  $\beta < 60^\circ$ .

But the requirement for a shell to be thin - the ratio of the wall thickness to the radius of curvature is much less than unity - is too vague to have a precise criterion. However, based on both experience and this vague requirement, we shall here provide an approximate guideline which may be quite helpful in selecting a cap size. From  $\lambda = 1.82 a/\sqrt{Rh}$  it is proposed  $\lambda > 2.5$  for a shell being thin. This proposed guideline is quite in line with the argument for deciding the critical arc length [3]. In summary, a shell is called thin and shallow if  $\lambda > 2.5$  and  $\beta < 60^\circ$ ; these are two basic guidelines adopted in this paper for forming a spherical cap from a hemispherical shell (Fig. 7).

Another important aspect concerning the buckling analysis of initially imperfect spherical shells is what is a better way of expressing initial imperfections. Determining the local radius over a critical arc length around the imperfect region as has been suggested in Ref. [3] is very hard to accomplish in practice, and for some occasions is almost impossible to carry out when the irregularity of unevenness is involved. One of the best ways to deal with this situation is by measuring departures from sphericity,  $W_i$  (Fig. 1), for a number of nodal points on a generic spoke. Accordingly, the initial imperfection at a point within the flat spot region (Fig. 8) may be approximated by

$$W_i = R(\cos \theta - \cos \frac{\phi}{2}) - R_1(\cos \gamma - \cos \frac{\alpha}{2}) \quad (16)$$

This approach poses a flexibility that any imperfection pattern including irregular distribution of deviations from sphericity can easily be measured and readily be adopted in governing equations for the theoretical analysis.

Figure 9 shows a one-dimensional finite-difference mesh superposed on the axisymmetric spherical cap domain; a clamped edge is assumed. An appropriate fixed number of evenly spaced nodal points are chosen in the flat spot region. Additional nodal points with the same even spacing are also distributed in the remaining perfect region. The number of nodal points in this region is varied depending on the size of the spherical cap selected.  $\lambda_0$  and  $\lambda$  appeared in this Figure represent the shallow region geometric parameters for the flat spot and the selected spherical cap, respectively.

Twelve hemispheres among 36 Series FS models listed in Table 1 are chosen for the present analysis. A well balanced choice on these test specimens is achieved by selecting every other two model according to the sequence of model number displayed in Table 1. For each model, the analysis is performed on a number of  $\lambda$  values for the purpose of verifying the local phenomenon on the collapse of initially imperfect spherical shells.

Numerical solutions in the form of buckling load versus geometric parameter of the selected spherical cap,  $q_{cr}/\lambda$ , are tabulated in Table 2. Also recorded in this Table are those of experiment and empirical method [3]. By comparing the values

of  $\lambda$  and  $\lambda_0$ , it seems that quite a wide range of various spherical cap sizes larger than the flat spot has been considered. From the values of  $(W_i)_{\max}/h$ , it also appears that quite a variety of imperfection magnitudes has been involved in these models.

The solution pattern emerged shows a tendency of a monotonic decreasing and then an increasing for  $q_{cr}$  against  $\lambda$ , having a small to moderate rate of change of  $q_{cr}$  with respect to  $\lambda$  for most cases. In each case, the spherical cap that yields a minimum  $q_{cr}$  value\* represents a shallow region of the hemisphere which is subjected to the least detrimental effect of clamping the edge. Therefore, this critical spherical cap may simulate the actual deformed (or damaged) area of the shell structure when the collapse occurs. Based on this argument, it is suggested that the buckling pressure of the critical spherical cap be taken as the theoretical collapse pressure for its associated hemispherical shell.

It should be very interesting to compare the critical spherical cap region with the actual deformed area of the collapsed model. A successful comparison will not only provide a strong evidence of the local phenomenon on the collapse of imperfect spherical shells, but also provide a strong support to the applicability of the spherical cap theory to deep imperfect spherical shell problems.

---

\*We may henceforth call the spherical cap which yields a minimum  $q_{cr}$  the "critical spherical cap," and designate its corresponding minimum  $q_{cr}$  as  $q_t$ , which stands for the theoretical buckling pressure for spherical shells under considerations.

For the purpose of references, two typical load vs central deflection curves are plotted in Figs. 10 and 11 for the critical spherical caps of Models FS-25 and FS-31, respectively. For the cap of Fig. 10, plastic yielding was set in at the load level of 2600 psi, but, for the case of FS-31 model, there was no evidence that plastic deformation has ever occurred.

The comparison between theoretical and experimental results shows that four models have an average  $q_t/q_{exp}$  value of 1.0375 while this value reduces to 0.886 for remaining eight. The comparison is regarded to be good, considering the fact that the flat spot models have abrupt change in curvature, which would not be true for imperfections in most practical shells and thus is considered as the case of severe imperfections. Taking this into account and other effects related to the clamped edge which is artificially introduced to the shell structure, we may disregard the difference of a less than 4% in buckling loads involved in those four models, and view theoretical results as the lower-bound solutions for imperfect spherical shells.

A similar comparison between empirical and experimental data gives an average  $q_E^1/q_{exp}$  value of 1.13 for a group of seven models and 0.963 for the remaining group. Based on similar reasons, empirical data may be treated as the upper-bound solutions for imperfect spherical shells under consideration.

In the empirical approach, the analysis is centered on a shallow spherical portion with a  $\lambda$  value of 2.2 which in some models falls within the flat spot region. A most striking

example may be referred to Model FS-31. Its flat spot poses a  $\lambda_0$  value of 4.17 compared with a shallow portion of  $\lambda = 2.2$  utilized in the analysis. Without taking the entire imperfect region into consideration may be a contributing factor, among others, responsible for the huge difference between its empirical and experimental buckling results - 747 psi vs 525 psi.

For very shallow spherical regions, say, with  $\lambda < 2.5$ , the detrimental effect of boundary conditions or secondary moments becomes more severe and tends to increase their rigidity, which may be a part of reasons to have them yield higher buckling loads than those of having larger  $\lambda$  values. This argument may be supported by the fact that the critical spherical caps employed in the present theoretical study, having  $\lambda$  values of ranging from 3.4 to 7.6, possess for most cases higher load-carrying capacities than their corresponding empirical values.

Generally speaking, the comparison among these three sets of results is surprisingly good. The good comparison suggests that initially imperfect spherical shells can be analyzed by using a much simpler mathematical model - the spherical cap - by which the analytic cost can be greatly reduced. At the same time, this also emphasizes the usefulness of the shallow spherical shell theory because it can be applied to solve important practical structural problems.

We shall here discuss some observations made in Refs. [4,5,6,11] concerning the influence of plastic yielding and initial imperfections. The first observation is that the initial

imperfection has a great impact on reducing the buckling strength of the shell structure, the degree of the impact increased with increase of the imperfection magnitude.

This observation may be confirmed by, for example, a comparison of results obtained for Models FS-13 and 22. Both shells are almost identical except for the local radius in the flat spot;  $R_1/R = 1.15$  for FS-13 and 1.4 for FS-22. The difference in local radii creates a difference in imperfection magnitudes:

$(W_i)_{\max}/h = 0.162$  and  $0.346$  for FS-13 and 22, respectively. As a result of this difference, FS-13 model with less severe imperfections yields a higher buckling load than FS-22: 910 psi vs 770 psi theoretically, or 1040 psi vs 718 psi experimentally.

The next observation is that plastic yielding also has a significant influence in reducing the buckling pressure of spherical shell structures, this influence increased with increase of the thickness-to-radius ratio [4,11,12]. This observation may be confirmed by, for example, comparing the results of Models FS-19 and 25. Both models are identical with a difference only in the wall thickness. For Model FS-19 of  $h/R = 0.0062$ , no plastic deformation ever occurs during the entire loading process, and hence, its buckling load (140 psi) is an elastic solution. On the other hand, Model FS-25 of  $h/R = 0.0304$ , having plastic yielding set in approximately at a load level of 2600 psi, yields an elastic-plastic buckling pressure of 3700 psi. The influence of plastic yielding increased with increase of the thickness-to-radius ratio is quite obvious.

### CONCLUSIONS

A finite difference method for the large deformation elastic-plastic buckling analysis of spherical caps developed in Ref. [4] is applied to predict the collapse strength of hemispherical shells with flat spots. Twelve out of 36 hemisphere models experimented in Ref. [3] are selected for the analysis. In each selected model, a number of shallow spherical regions containing flat spots and with clamped edges are chosen from its domain. The critical spherical cap is the one, among those chosen, which yields a minimum buckling pressure; this minimum value is taken as the theoretical buckling load for its associated imperfect hemispherical shell.

Present theoretical solutions are in good agreement with those of experiment and empirical method [3]. Compared with those of experiment, present results represent lower-bound solutions to these shell problems, having an average of nearly 90% accuracy, while empirical data provide upper-bound solutions with an average of about only 13% in error.

Good comparison among these three sets of results suggests that initially imperfect spherical shells can be analyzed by using a much simpler mathematical model - spherical cap - by which the analytical cost can be greatly reduced. At the same time, this good comparison also emphasizes the usefulness of the shallow spherical shell theory because of its applicability to important practical structural problems. This comparison

also serves to justify the efforts made in so many publications for the development of shallow spherical shell theories.

An important implication also emerged from this comparison is that the collapse of spherical shells is primarily a local phenomenon and therefore critically dependent on local geometry, a view also shared in Ref. [3]. This implication makes it clear that the presence of initial imperfections should be fully taken into consideration in any large deformation analysis before such analysis can be expected to quantitatively predict the collapse strength of practical shells.

Present solutions together with experimental and empirical data confirm a general belief that the initial imperfection plays an important role in reducing the collapse strength of shell structures, the influence of the imperfection increased with increase of its magnitude [4,5,6,11]. It is also found that plastic yielding has a significant effect of weakening spherical shells, the degree of this effect increased with increase of the thickness-to-radius ratio. This is a finding also observed in Refs. [4,11,12].

#### ACKNOWLEDGMENTS

The author would like to express his deep appreciation to Dr. N. Perrone, Office of Naval Research, for his valuable discussion. His appreciation is also extended to Mr. T. J. Kiernan, David Taylor Naval Ship Research and Development Center, for his providing useful information for the test specimens.

Table 1. Dimensions of Series FS hemispherical shell models  
(Fig. 5)\*

Model	$h_1$ in.	$h_2$ in.	$\alpha$ deg.	$R_1$ in.	$b$ in.	$g$ in.	$2 R_{oc}$ in.	$2 R_{of}$ in.	$\frac{R_1}{K}$
FS-1	0.0061	0.0062	10	1.138	0.022	0.044	1.638	1.688	1.4
FS-2	0.0064	0.0064	10	1.138	0.022	0.044	1.638	1.688	1.4
FS-3	0.0104	0.0104	10	1.138	0.028	0.055	1.648	1.702	1.4
FS-4	0.0104	0.0104	10	1.138	0.028	0.055	1.648	1.702	1.4
FS-5	0.0162	0.0162	10	1.138	0.079	0.079	1.661	1.751	1.4
FS-6	0.0159	0.0161	10	1.138	0.079	0.079	1.661	1.751	1.4
FS-7	0.0247	0.0249	10	1.138	0.090	0.090	1.681	1.827	1.4
FS-8	0.0499	0.0400	10	1.138	0.115	0.115	1.717	1.967	1.4
FS-9	0.0694	0.0696	10	1.138	0.154	0.154	1.789	2.338	1.4
FS-10	0.0062	0.0052	20	0.934	0.022	0.044	1.638	1.688	1.15
FS-11	0.0063	0.0063	20	0.934	0.022	0.044	1.638	1.688	1.15
FS-12	0.0101	0.0101	20	0.934	0.028	0.055	1.648	1.702	1.15
FS-13	0.0102	0.0102	20	0.934	0.028	0.055	1.648	1.702	1.15
FS-14	0.0159	0.0161	20	0.934	0.079	0.079	1.661	1.751	1.15
FS-15	0.0159	0.0160	20	0.934	0.079	0.079	1.661	1.751	1.15
FS-16	0.0250	0.0250	20	0.934	0.090	0.090	1.681	1.827	1.15
FS-17	0.0399	0.0399	20	0.934	0.115	0.115	1.717	1.967	1.15
FS-18	0.0694	0.0697	20	0.934	0.154	0.154	1.789	2.338	1.15
FS-19	0.0050	0.0051	20	1.138	0.022	0.044	1.638	1.688	1.4
FS-20	0.0061	0.0061	20	1.138	0.022	0.044	1.638	1.688	1.4
FS-21	0.0102	0.0102	20	1.138	0.028	0.055	1.648	1.702	1.4
FS-22	0.0104	0.0103	20	1.138	0.028	0.055	1.648	1.702	1.4
FS-23	0.0154	0.0160	20	1.138	0.079	0.079	1.661	1.751	1.4
FS-24	0.0157	0.0161	20	1.138	0.079	0.079	1.661	1.751	1.4
FS-25	0.0251	0.0251	20	1.138	0.090	0.090	1.681	1.827	1.4
FS-26	0.0400	0.0400	20	1.138	0.115	0.115	1.717	1.967	1.4
FS-27	0.0694	0.0699	20	1.138	0.154	0.154	1.789	2.338	1.4
FS-28	0.0061	0.0061	30	1.138	0.022	0.044	1.638	1.688	1.4
FS-29	0.0063	0.0063	30	1.138	0.022	0.044	1.638	1.688	1.4
FS-30	0.0104	0.0104	30	1.138	0.028	0.055	1.648	1.702	1.4
FS-31	0.0104	0.0104	30	1.138	0.028	0.055	1.648	1.702	1.4
FS-32	0.0161	0.0163	30	1.138	0.079	0.079	1.661	1.751	1.4
FS-33	0.0155	0.0159	30	1.138	0.079	0.079	1.661	1.751	1.4
FS-34	0.0245	0.0249	30	1.138	0.090	0.090	1.681	1.827	1.4
FS-35	0.0397	0.0397	30	1.138	0.115	0.115	1.717	1.967	1.4
FS-36	0.0700	0.0701	30	1.138	0.154	0.154	1.789	2.338	1.4

\*The data listed here are originally recorded in Ref. [3].

Table 2. Summary of geometric parameters and collapse pressures for Series FS hemispherical shell models

Model	h in	R in	R <sub>1</sub> in	φ	$\frac{(W_i)_{max}}{h}$	λ <sub>0</sub>	a	$\frac{q_{cr}}{\lambda}$	b	q <sub>t</sub> c psi	q <sub>exp</sub> d psi	q <sub>E</sub> <sup>i</sup> d psi	q <sub>t</sub> psi	q <sub>E</sub> <sup>i</sup> psi	q <sub>t</sub> psi	q <sub>E</sub> <sup>i</sup> psi	q <sub>t</sub> psi	q <sub>E</sub> <sup>i</sup> psi
1	.0061	.8156	1.141	10	.146	1.833	560 2.64	340 4.25	380 5.05	460 5.83	328	354	1.04	1.08				
4	.0104	.8177	1.1432	10	.086	1.046	1450 2.65	1090 3.87	1100 4.47	1050	1230	1190	.854	.967				
7	.0247	.8249	1.1504	10	.037	.916	4800 3.47	4400 3.96	4600 4.4	4400	4280	4125	1.028	.964				
10	.0062	.8156	.9371	20	.267	3.62	340 4.37	340 5.12	380 6.51	340	388	397	.876	1.023				
13	.0102	.8175	.94	20	.162	2.83	960 3.41	910 4.0	1020 5.14	910	1040	1030	.875	.99				
16	.0250	.825	.947	20	.068	1.81	5000 2.61	3900 3.38	4100 4.87	3900	4215	4025	.925	.955				
19	.005	.815	1.1405	20	.714	4.0	140 4.87	140 5.7	150 7.23	140	153	175	.915	1.144				
22	.0104	.8177	1.1432	20	.346	2.8	840 3.38	770 4.53	820 5.10	770	718	747	1.072	1.04				
25	.0251	.8251	1.1506	20	.145	1.81	4800 2.6	3700 3.37	3800 4.86	4000 5.56	3880	3640	.954	.938				
28	.0061	.8156	1.141	30	1.334	5.44	180 6.55	160 7.64	180 9.75	160	228	260	.702	1.14				
31	.0104	.8177	1.143	30	.786	4.17	570 5.02	530 6.68	570 7.48	530	525	747	1.01	1.423				
34	.0248	.8249	1.1504	30	.334	2.73	2800 3.87	2800 4.98	3000 6.01	2800	2850	3025	.983	1.061				

a λ<sub>0</sub> is the geometric parameter for the flat spot (Fig. 9).

b q<sub>cr</sub>/λ are the collapse pressure of the spherical cap against its own geometric parameter; q<sub>cr</sub> (psi).

c q<sub>t</sub>, whose value equals to (q<sub>cr</sub>)<sub>min</sub>, is taken as the theoretical collapse pressure for the hemispherical shell model under consideration.

d q<sub>exp</sub> and q<sub>E</sub><sup>i</sup> are the experimental and empirical collapse pressures, respectively [3]; q<sub>E</sub><sup>i</sup> is obtained from Eq.(15).

REFERENCES

- [ 1] Timoshenko, S., "Theory of Elasticity," McGraw-Hill Co., Inc., New York (1936).
- [ 2] Fung, Y. C. and Seckler, E. E., "Instability of Thin Elastic Shells," Proceedings of the first symposium on on naval structural mechanics (1960).
- [ 3] Krenzke, M. A. and Kiernan, T. J., "The Effect of Initial Imperfections on the Collapse Strength of Deep Spherical Shells," David Taylor Model Basin Report 1757 (February 1965).
- [ 4] Kao, R., "Large Deformation Elastic-Plastic Buckling Analysis of Spherical Caps with Initial Imperfections," To appear in Computers and Structures.
- [ 5] Koga, T. and Hoff, N. J., "The Axisymmetric Buckling of Initially Imperfect Complete Spherical Shells," Internal Journal Solids and Structures (July 1969).
- [ 6] Kao, R. and Perrone, N., "Asymmetric Buckling of Spherical Caps with Asymmetric Imperfections," Journal of Applied Mechanics, 38 (1) (March 1971).
- [ 7] Krenzke, M. A. and Kiernan, T. J., "Tests of Stiffened and Unstiffened Machined Spherical Shells under External Hydrostatic Pressure," David Taylor Model Basin Report 1741 (August 1963).
- [ 8] Krenzke, M. A., "Tests of Machined Deep Spherical Shells under External Hydrostatic Pressure," David Taylor Model Basin Report 1601 (May 1962).
- [ 9] Krenzke, M. A., "The Elastic Buckling Strength of Near-Perfect Deep Spherical Shells with Ideal Boundaries," David Taylor Model Basin Report 1713 (July 1963).
- [10] Perrone, N. and Kao, R., "A General Nonlinear Relaxation Technique for Solving Nonlinear Problems in Mechanics," J. of Applied Mechanics, 38 (2) (June 1971), pp. 371-376.
- [11] Kao, R., "Nonlinear Dynamic Buckling of Spherical Caps with Initial Imperfections," To appear in Computers and Structures.
- [12] Marcal, P. V., "Large Deflection Analysis of Elastic-Plastic Shells of Revolution," AIAA J., 8 (9) (September 1970).

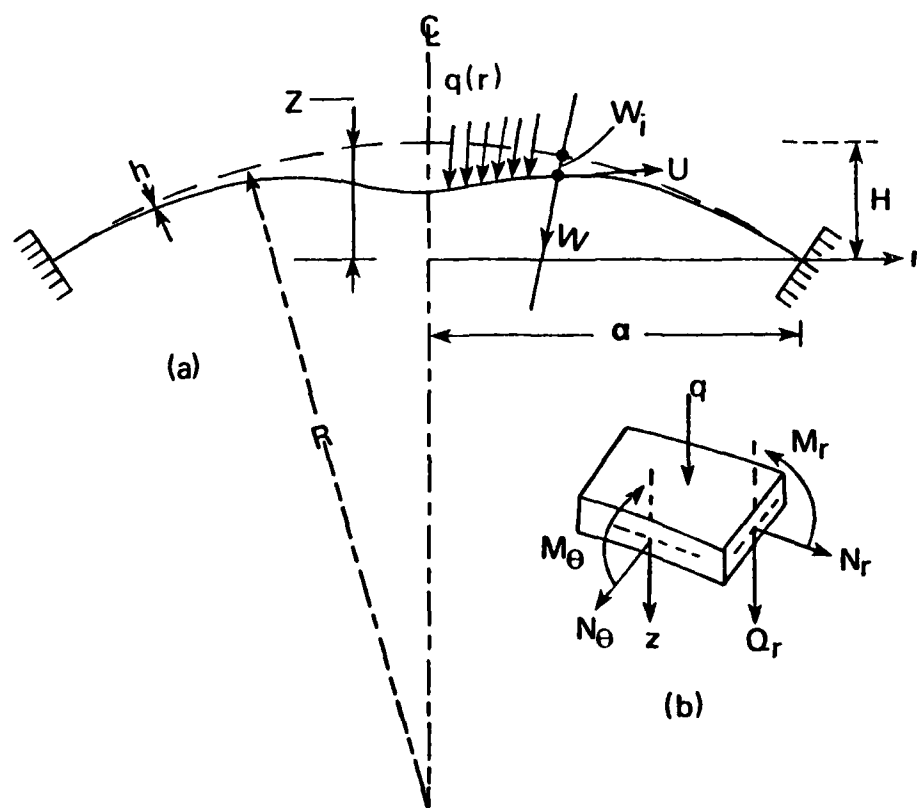


Fig.1- Geometry, stress resultants and moments for axisymmetric clamped spherical cap with initial imperfection.

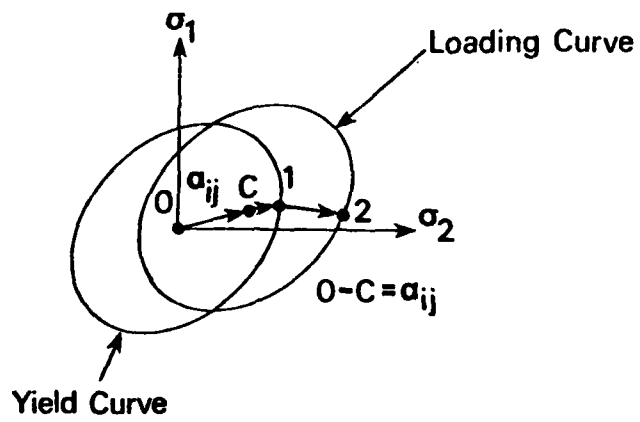


Fig. 2 - Kinematic hardening in plane stress.

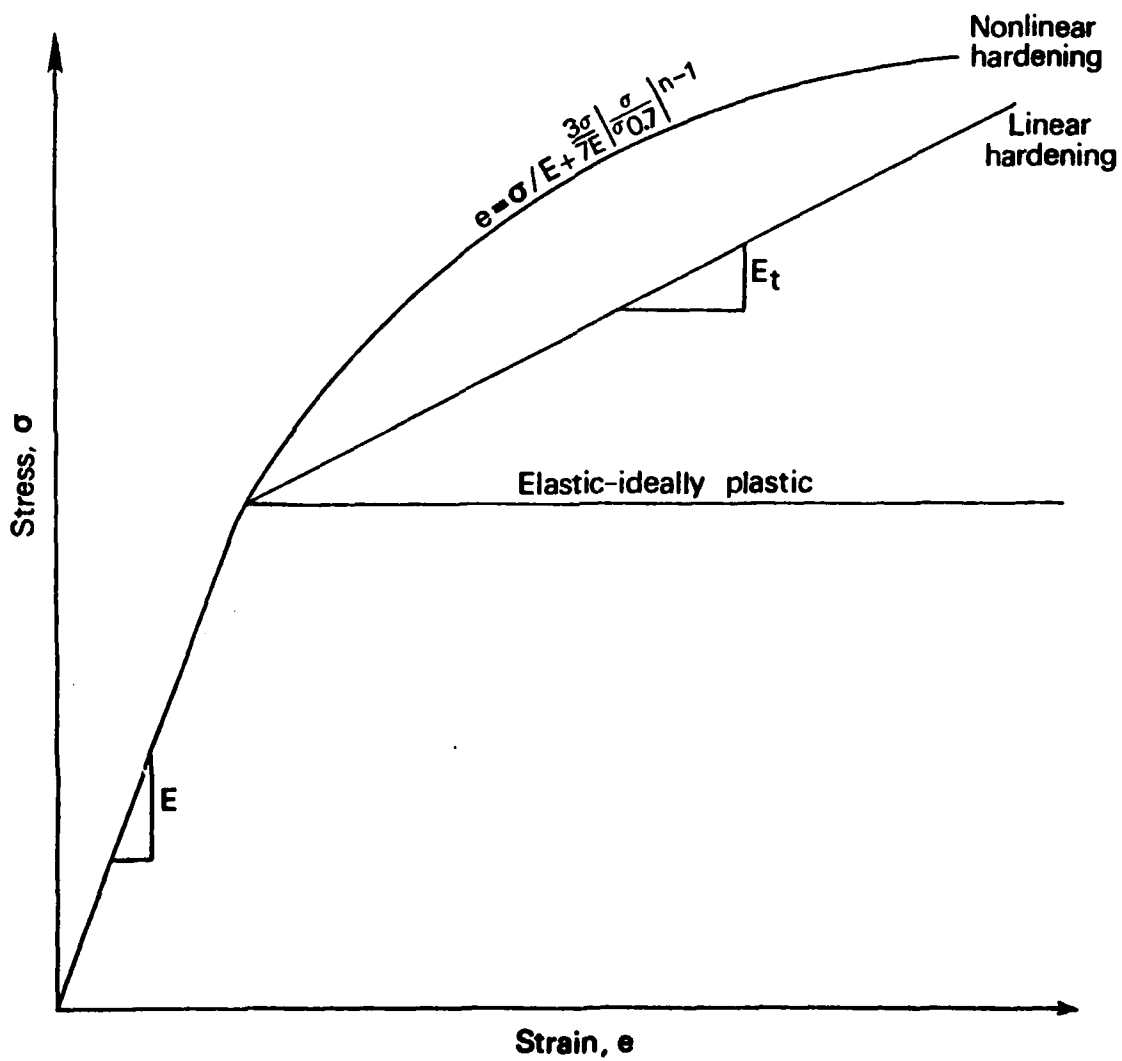


Fig. 3- Nonlinear stress-strain curves  
(three types of hardening).

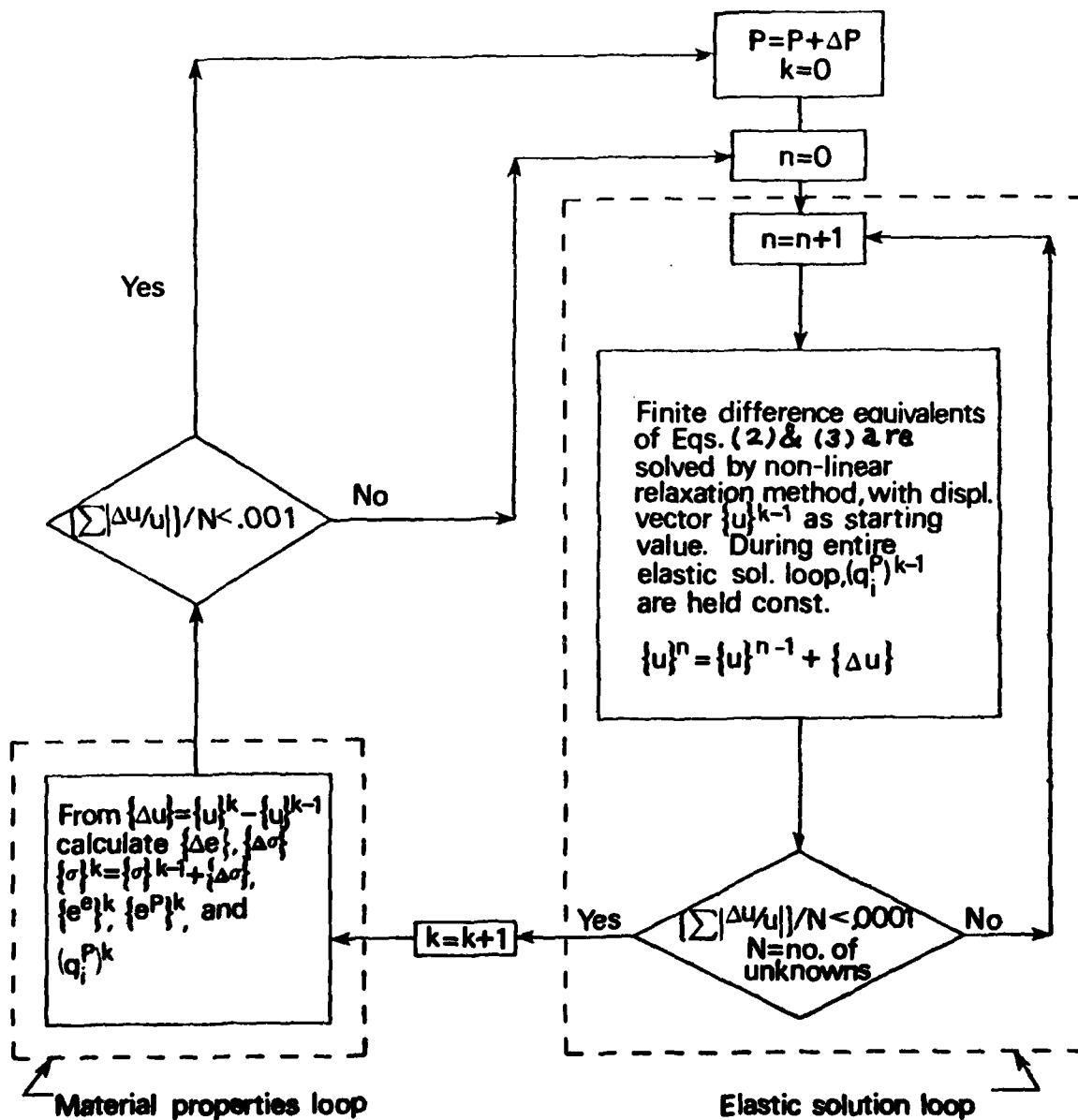


Fig. 4 - Iteration procedure for large deformation elastic-plastic problems.

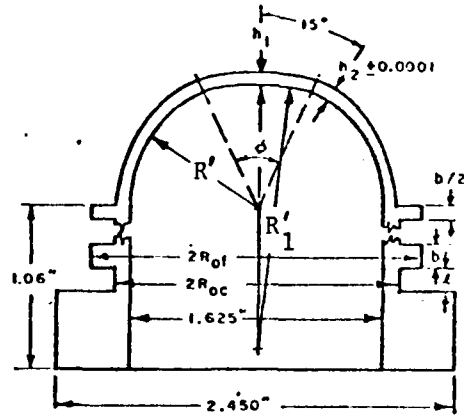


Fig. 5-Geometry of Series FS hemispherical shell models.

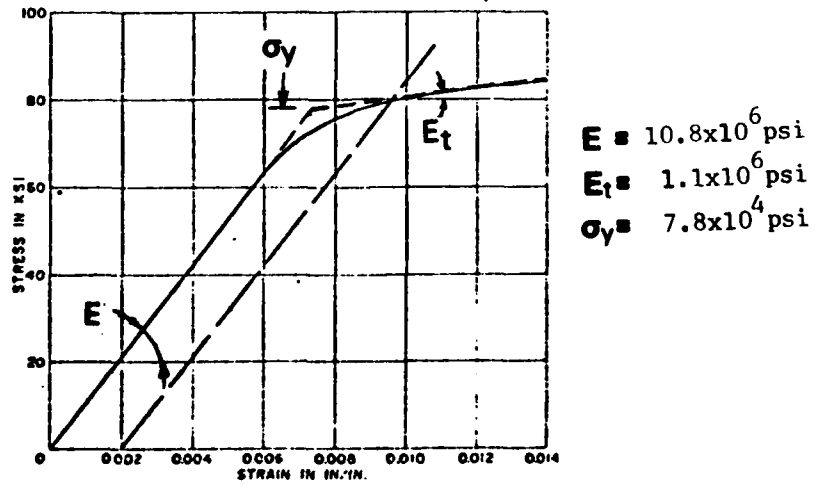


Fig. 6-Typical stress-strain curve for 7075 - T6 aluminum alloy.

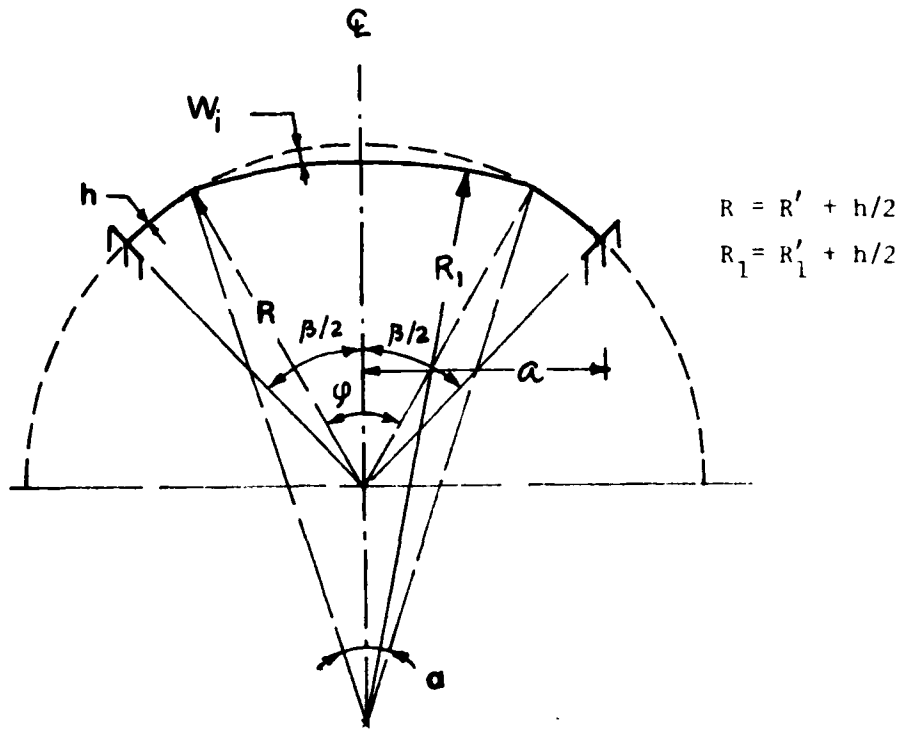


Fig. 7 - Spherical cap obtained from an initially imperfect hemisphere.

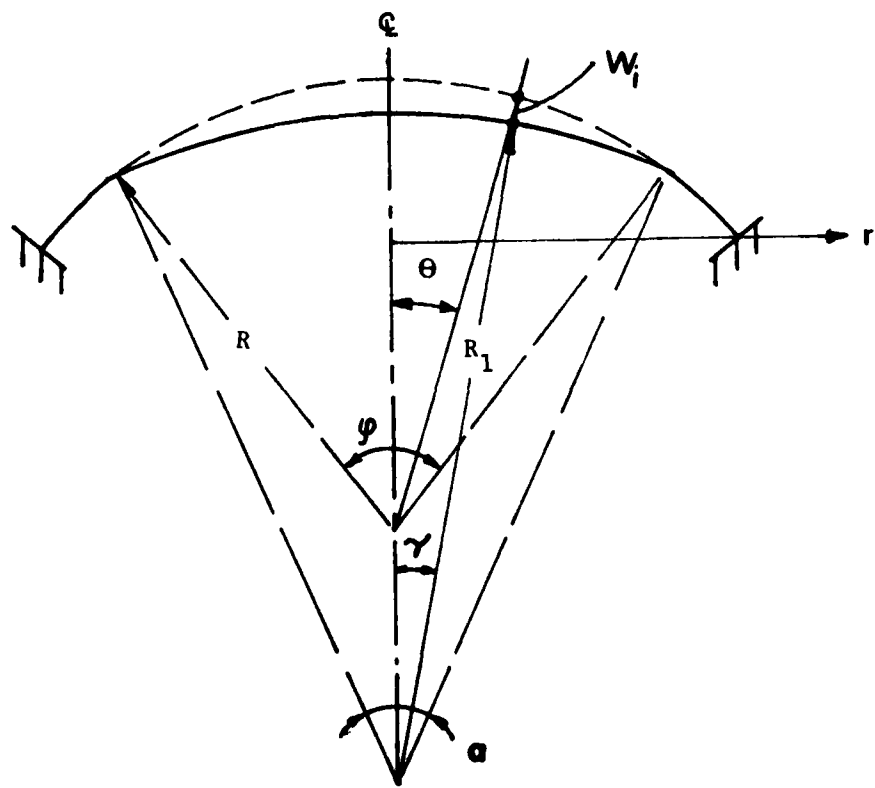


Fig. 8 - Determination of imperfections for a spherical cap with flat spot.

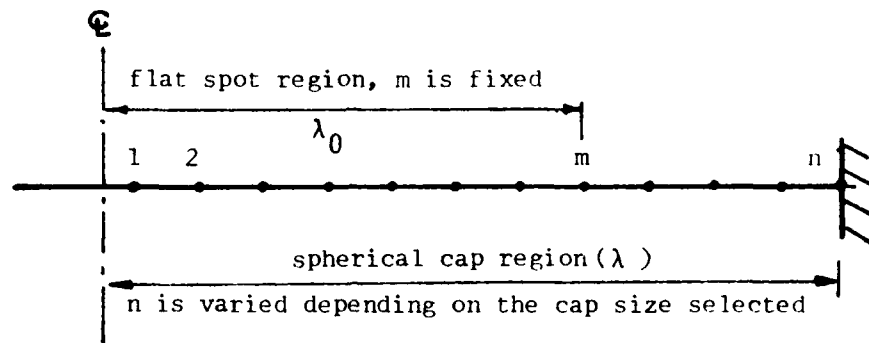


Fig. 9 - One dimensional finite-difference mesh on axisymmetric spherical cap domain.

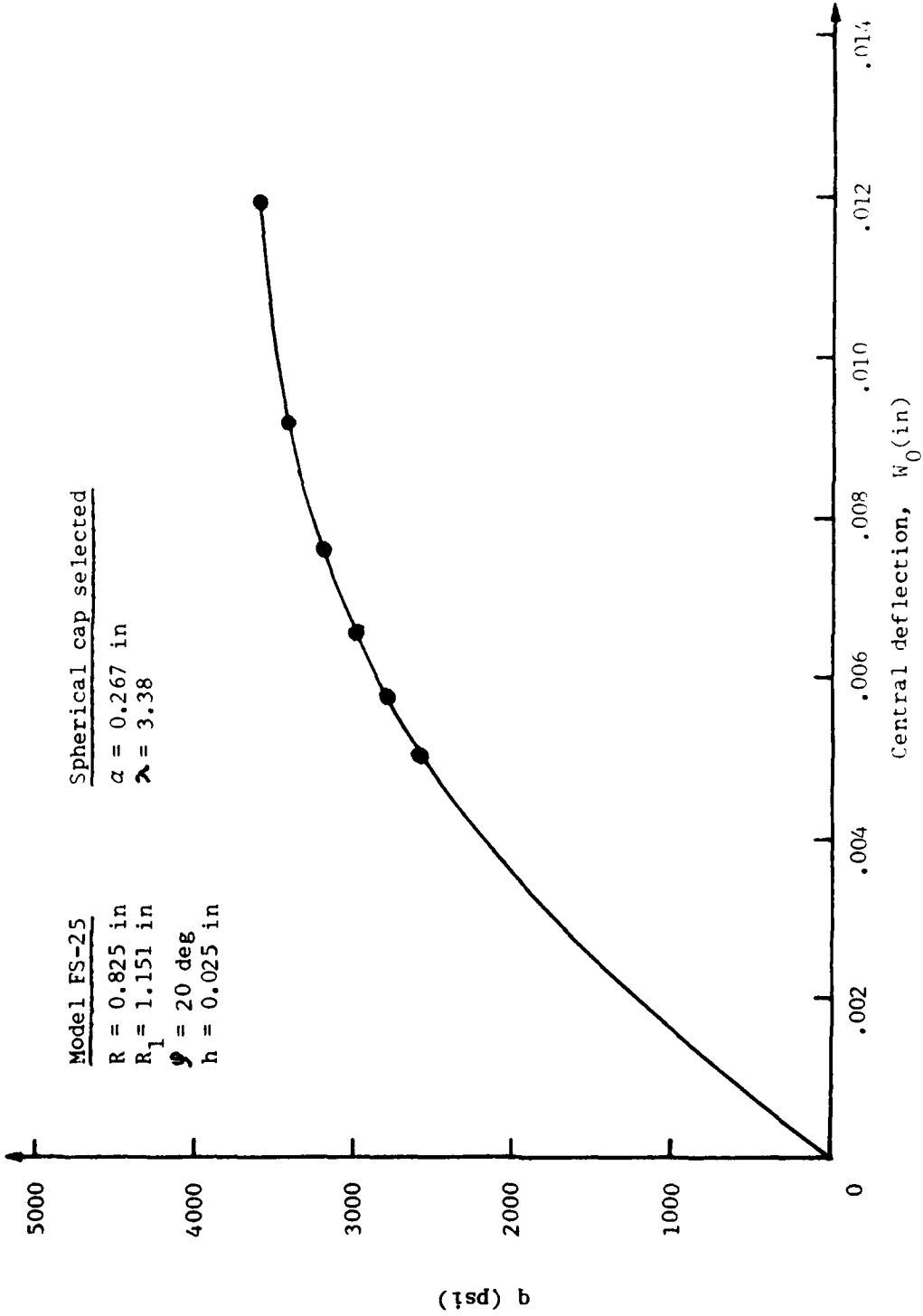


Fig. 10 - Elastic-plastic buckling of a clamped spherical cap ( $\lambda = 3.38$ ) with flat spot selected from Model FS-25 (load vs central deflection).

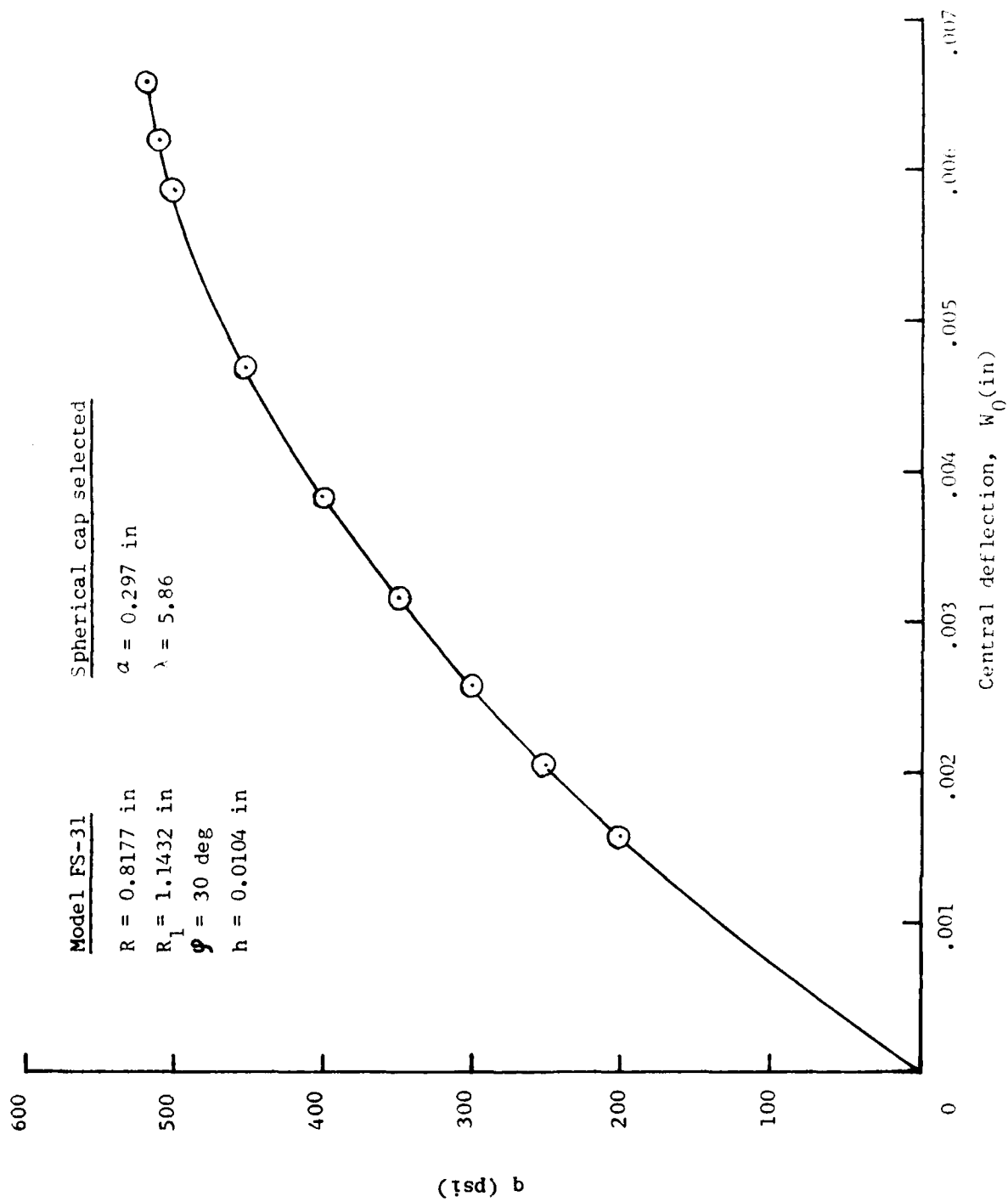


Fig. 11 - Elastic buckling of a clamped spherical cap ( $\lambda = 5.86$ ) with flat spot selected from Model FS-31 (load vs central deflection).

REPORT DOCUMENTATION PAGE		READ INSTRUCTIONS BEFORE COMPLETING FORM
1. REPORT NUMBER	2. GOVT ACCESSION NO. AD-AC86 006	3. RECIPIENT'S CATALOG NUMBER
4. TITLE (and Subtitle) A COMPARATIVE STUDY ON THE ELASTIC-PLASTIC COLLAPSE STRENGTH OF IMPERFECT DEEP SPHERICAL SHELLS		5. TYPE OF REPORT & PERIOD COVERED
7. AUTHOR Robert Kao		6. PERFORMING ORG. REPORT NUMBER
9. PERFORMING ORGANIZATION NAME AND ADDRESS The George Washington University School of Engineering and Applied Science Washington, D.C. 20052		8. CONTRACT OR GRANT NUMBER(s) NAVY 00014-75-C-0946
11. CONTROLLING OFFICE NAME AND ADDRESS Office of Naval Research Arlington, Virginia 22217		10. PROGRAM ELEMENT PROJECT TASK AREA & WORK UNIT NUMBERS
14. MONITORING AGENCY NAME & ADDRESS (if different from Controlling Office)		12. REPORT DATE February 1980
		13. NUMBER OF PAGES 40 pages
		15. SECURITY CLASS. (of this report) UNCLASSIFIED
		16. DECLASSIFICATION/DOWNGRADING SCHEDULE
16. DISTRIBUTION STATEMENT (of this Report) APPROVED FOR PUBLIC RELEASE: DISTRIBUTION UNLIMITED		
17. DISTRIBUTION STATEMENT (of the abstract entered in Block 20, if different from Report)		
18. SUPPLEMENTARY NOTES		
19. KEY WORDS (Continue on reverse side if necessary and identify by block number) Collapse strength      Initial imperfections      Empirical method Large deformation      Spherical caps      Flat spots Plastic deformation      Finite differences Kinematic hardening      Deep spherical shells		
20. ABSTRACT (Continue on reverse side if necessary and identify by block number) Twelve uniformly loaded hemispherical shells with flat spots are analyzed by a large deformation elastic-plastic spherical cap theory. For each hemisphere a number of shallow spherical regions are selected from its domain. One of these shallow regions yields a minimum buckling load; this minimum value is taken as the theoretical buckling pressure for the hemisphere under consideration. Present solutions compare quite favorably with existing experimental and empirical results.		

DD FORM 1473  
1 JAN 73EDITION OF 1 NOV 68 IS OBSOLETE  
S. N. 0102-014-6601

SECURITY CLASSIFICATION OF THIS PAGE (When Data Entered)

# THE GEORGE WASHINGTON UNIVERSITY

BENEATH THIS PLAQUE  
IS BURIED  
A VAULT FOR THE FUTURE  
IN THE YEAR 2036

THE STORY OF ENGINEERING IN THIS YEAR OF THE PLACING OF THE VAULT AND  
ENGINEERING HOPES FOR THE TOMORROWS AS WRITTEN IN THE RECORDS OF THE  
FOLLOWING GOVERNMENTAL AND PROFESSIONAL ENGINEERING ORGANIZATIONS AND  
THOSE OF THIS GEORGE WASHINGTON UNIVERSITY.

BOARD OF COMMISSIONERS DISTRICT OF COLUMBIA  
UNITED STATES ATOMIC ENERGY COMMISSION  
DEPARTMENT OF THE ARMY UNITED STATES OF AMERICA  
DEPARTMENT OF THE NAVY UNITED STATES OF AMERICA  
DEPARTMENT OF THE AIR FORCE UNITED STATES OF AMERICA  
NATIONAL ADVISORY COMMITTEE FOR AERONAUTICS  
NATIONAL BUREAU OF STANDARDS U.S. DEPARTMENT OF COMMERCE  
AMERICAN SOCIETY OF CIVIL ENGINEERS  
AMERICAN INSTITUTE OF ELECTRICAL ENGINEERS  
THE AMERICAN SOCIETY OF MECHANICAL ENGINEERS  
THE SOCIETY OF AMERICAN MILITARY ENGINEERS  
AMERICAN INSTITUTE OF MINING & METALLURGICAL ENGINEERS  
DISTRICT OF COLUMBIA SOCIETY OF PROFESSIONAL ENGINEERS, INC.  
THE INSTITUTE OF RADIO ENGINEERS, INC.  
THE CHEMICAL ENGINEERS CLUB OF WASHINGTON  
WASHINGTON SOCIETY OF ENGINEERS  
FAULKNER KINGSBURY & STENHOUSE - ARCHITECTS  
CHARLES H. TOMPKINS COMPANY - BUILDERS  
SOCIETY OF WOMEN ENGINEERS  
NATIONAL ACADEMY OF SCIENCES NATIONAL RESEARCH COUNCIL

THE PURPOSE OF THIS VAULT IS INSPIRED BY AND IS DEDICATED TO  
CHARLES HOOK TOMPKINS, DOCTOR OF ENGINEERING  
BECAUSE OF HIS ENGINEERING CONTRIBUTIONS TO HIS UNIVERSITY, TO HIS  
COMMUNITY, TO HIS NATION, AND TO OTHER NATIONS.

BY THE GEORGE WASHINGTON UNIVERSITY

ROBERT W. FLEMING

CHAIRMAN OF THE BOARD OF TRUSTEES

GLOYD H. MARVIN

PRESIDENT

JUNE 19, 1955

To cope with the expanding technology, our society must be assured of a continuing supply of rigorously trained and educated engineers. The School of Engineering and Applied Science is completely committed to this objective.

DATE  
FILMED  
-8